SHAFIQUZZAMAN MD (Orcid ID: 0000-0002-4668-0983)
Biswas Soma (Orcid ID: 0000-0002-1427-2678)
Liu Huijuan (Orcid ID: 0000-0002-8801-4815)

The non-canonical BMP signaling pathway plays an important role in club cell regeneration

Md Shafiquzzaman[1,2,3], Soma Biswas[1], Ping Li[1], Yuji Mishina[4], Baojie Li[1,5], and Huijuan Liu[1, 2, *]

[1]Bio-X Institutes, Key Laboratory for the Genetics of Developmental and Neuropsychiatric Disorders, Ministry of Education, Shanghai Jiao Tong University, Shanghai 200240, China.

[2]Metabolic Bone Disease and Genetics Research Unit, Department of Osteoporosis and Bone Diseases, Shanghai Jiao Tong University Affiliated Sixth People's Hospital, Shanghai, China.

[3]National Institute of Biotechnology, Ministry of Science and Technology, Dhaka 1349, Bangladesh.

[4]Department of Biologic & Materials Sciences, School of Dentistry, University of Michigan, 1011N, University Ave., Ann Arbor, MI, 48109, USA.

[5]Center for Traditional Chinese Medicine and Stem Cell Research, the Chengdu University of Traditional Chinese Medicine, Sichuan, China.

[*]Correspondence: Huijuan Liu, Ph. D.,
Bio-X Institutes, Shanghai Jiao Tong University, Shanghai 200240, China
Tel: 86-21-34207286; Email: liuhj@sjtu.edu.cn

Running title: mechanisms of club cell regeneration

This is the author manuscript accepted for publication and has undergone full peer review but has not been through the copyediting, typesetting, pagination and proofreading process, which may lead to differences between this version and the Version of Record. Please cite this article as doi: 10.1002/stem.3125

Key Words: Club cells, Bronchiolar epithelium, Club cell regeneration, Non-canonical BMP pathway, Tak1-p38MAPK, Prrx1.

Abstract

The bronchiole is a major site for the development of several life-threatening disorders including chronic obstructive pulmonary disease and lung adenocarcinomas. The bronchiolar epithelium is composed of club cells and ciliated epithelial cells, with club cells serving as progenitor cells. Presently, the identity of the cells involved in regeneration of bronchiolar epithelium and the underlying mechanisms remain incompletely understood. Here we show that Prrx1, a homeobox transcription factor, can mark club cells in adult mice during homeostasis and regeneration. We further show that the non-canonical signaling pathway of BMPs, BMPR1A-Tak1-p38MAPK plays a critical role in club cell regeneration. Ablation of *Bmpr1a*, *Tak1*, or *Mapk14* (encoding p38α) in $Prrx1^+$ club cells caused minimal effect on bronchiolar epithelium homeostasis, yet it resulted in severe defects in club cell regeneration and bronchiole repair in adult mice. We further show that this pathway supports proliferation and expansion of the regenerating club cells. Our findings thus identify a marker for club cells and reveal a critical role for the BMP non-canonical pathway in club cell regeneration.

Introduction

The respiratory system is developed from the ventral foregut endoderm cells marked by Nkx2-1 in mouse [1, 2]. By E16.5, the lung buds form a tree-like architecture of airways with thousands of terminal tubules [3], which generate numerous epithelial sacs that later develop into alveoli [4]. In adult mice, the respiratory system displays low turnover rate [2]. Yet, it has great regeneration potentials in response to injuries caused by influenza virus infection, toxic chemical inhalation or other insults. In trachea, $p63^+$ basal cells can regenerate ciliated and secretory epithelial cells [5]. In small airways (bronchioles), $Scgb1a1^+$ (Uteroglobin) club cells self-renew and give rise to ciliated cells and contribute to repair of bronchiolar epithelium [6-9]. Earlier studies have suggested that club cell population is heterogenous and a portion of $Scgb1a1^+$ club cells, termed variant club cells, are stem cells [8, 10, 11]. Most recently, Upk3a has also been proposed to identify a rare subset of club cells with differentiation potentials [12]. In alveoli, type II cells (AEC2) act as stem cells to produce both type I and II alveolar cells [13, 14].

The BMP family members play key roles in lung development and homeostasis [4, 15-19]. The signal transduction cascade is initiated when BMPs bind to BMP receptor I (BMPRI) and II (BMPRII), which are serine/threonine kinases [20]. The constitutively active BMPRII then phosphorylates and activates BMPRI, which in turn phosphorylates Smad 1/5/8. Smad 1/5/8 associates with Smad4 and translocates to the nucleus where they function as transcription activator or repressor. Previous studies have shown that BMP4 regulates branching

morphogenesis and proximal-distal differentiation of lung endoderm [15, 19]. Ectopic expression of BMP4 or deletion of BMP antagonists in lung epithelium causes defects in lung development [17, 19], whereas inactivation of *Bmpr1a* and *Bmpr1b* results in tracheal agenesis [16]. In addition, *Smad1* knockout causes defects in lung branching and epithelium proliferation and differentiation [21, 22].

BMPs also activate non-canonical pathways that include Tak1 and MAPKs [23-25]. During mouse lung development, *Mapk14* (encoding *p38α*) is expressed as early as E10.5 and is involved in budding/branching, proliferation and differentiation of epithelial progenitor cells at the distal tips of the endoderm [26]. Ablation of *Mapk14* caused neonatal lethality, accompanied by abnormal alveolar structures and massive deposition of hematopoietic cells in the lung [27]. Postnatal deletion of *Mapk14* in the whole animal impaired proliferation and differentiation of lung stem and progenitor cells [28].

In addition to controlling embryonic lung development, BMP signaling pathway also regulates postnatal lung homeostasis and repair [29, 30]. A recent study showed that inhibition of BMP signaling promoted basal cell proliferation but not cell fate determination while BMP4 inhibited both basal cell proliferation and differentiation [31]. BMPs also play similar roles in AEC2 in response to pneumonectomy [32], where BMPs keep stem cells in a quiescent state. A transient up-regulation of BMP inhibitors during repair promotes cell proliferation and facilitates the repair process. However, the functions of the BMP non-canonical pathways in lung homeostasis and regeneration are less investigated and remain

elusive.

Club cells secrete uteroglobin, surfactant, and other proteins to protect the bronchiolar lining cells and to detoxify inhaled harmful substances while the ciliated cells pump fluid, which carries dust and germs, in or out of the bronchiolar lumen. Moreover, the bronchial and bronchioles are the major sites for development of chronic obstructive pulmonary disease and lung adenocarcinomas [33, 34]. Yet, the identity of the progenitor club cells and the mechanisms by which these cells regenerate bronchiolar epithelium remain incompletely understood. Here, our lineage tracing studies and conditional gene knockout mouse experiments identify Prrx1 as a marker for club cells and provide genetic evidence that the BMPR1A-Tak1-p38MAPK pathway plays an indispensable role in regeneration of bronchiolar epithelium by promoting club cell proliferation and expansion.

Materials and Methods

Mice

The *Rosa-tdTomato* and the transgenic *Prrx1-Cre* mice were purchased from the Jackson Laboratory. They were mated to obtain the *Prrx1-Cre; Rosa-tdTomato* mice. The transgenic *Prrx1-CreERT* mice were generated in Shunichi Murakami's lab [35], the floxed *Bmpr1a* mice were generated in Yuji Mishina's lab [36] and *Tak1*$^{f/f}$ mice were generated in Michael D. Schneider's lab. *Bmpr1a*$^{f/f}$ and *Tak1*$^{f/f}$ mice were crossed with *Prrx1-CreERT* mice to generate *Prrx1-CreERT; Bmpr1a*$^{f/f}$ and *Prrx1-CreERT; Tak1*$^{f/f}$ mice, in which *Bmpr1a* and *Tak1* was deleted after tamoxifen administration, respectively. The *Mapk14*$^{f/f}$ mouse line was generated in Dr. Yibin Wang's laboratory at UCLA and it was bred with the *Prrx1-Cre* mice to get the *Prrx1-Cre; Mapk14*$^{f/f}$ mice. The C57BL6 mice were purchased from the Charles River Laboratories.

All animals were bred and housed in the specific pathogen-free (SPF) facility of Bio-X institutes, Shanghai Jiao Tong University and food and water were provided *ad libitum*. Animal experimentations in this study were performed following the recommendations of the National Research Council Guide for Care and Use of Laboratory Animals, with all the experimental protocols approved by the Institutional Animal Care and Use Committee of Shanghai Jiao Tong University, China [SYXK (SH) 2011–0112].

Naphthalene (NA) administration

NA (Sigma-Aldrich) was dissolved in corn oil and a single dose was administered by intraperitoneal (i.p) injection (280 mg/kg body weight). Lung tissues were collected on day 3 and 7 post NA-treatment and processed for analyses.

Tamoxifen (TAM) administration

TAM (T5648, Sigma-Aldrich, St. Louis, MO, USA) powder was dissolved in corn oil at a concentration of 10 mg/ml and was kept foil-wrapped to protect from light. TAM was administered intraperitoneally at a dose of 100 mg/kg body weight on every other day for a total of 3 doses.

Tissue processing and histology

Mice were anesthetized by administration of avertin (2.5% tribromoethanol) through i.p injection. Chest cavity was opened surgically and 0.9% normal saline was used for perfusion through both left and right ventricle. The trachea was ligated after inflating lungs with 1.5 ml of 4% paraformaldehyde (PFA, pH 7.4) in PBS through the trachea. Heart and lungs were removed en bloc and further fixated overnight in 4% PFA at 4°C. For cryosections, superior lobe of right lung was removed after overnight fixation and embedded in OCT after dehydrating in graded sucrose solution and cryomicrotome (Leica CM3050S) was used to cut 4 µm thick sections. For paraffin sections, the left lung was removed, dehydrated in graded ethanol series, cleared in xylene, embedded in paraffin and 4 µm thick sections were cut using Leica RM2255 microtome.

Immunofluorescence

Paraffin sections were deparaffinized in xylene and rehydrated in graded ethanol series. Antigen retrieval was performed using 10 mM sodium citrate buffer (pH 6.0). Tissue sections were permeabilized with 0.1% Triton X-100 for 30 min at room temperature, blocked with 10% goat serum (in PBS) for 1 hour at room temperature (RT) and then incubated overnight with primary antibodies at 4°C. On the next day, tissue sections were incubated with secondary antibodies at 37°C for 1 hour and then mounted using SlowFade Gold antifade mountant (Invitrogen). DAPI (Invitrogen) was used to stain the nuclei. Primary antibodies used in this study are: Scgb1a1 (Abcam, ab40873, 1:750), α-acetylated Tubulin (Sigma-Aldrich, T7451, 1:600), and Ki67 (Abcam, ab15580, 1:100). Secondary antibodies used are: Alexa Fluor 488-goat anti-rabbit and Alexa Fluor 546-goat anti-mouse (both from Invitrogen, 1:100). Images were captured using Nikon Eclipse 80i microscope (Nikon Instruments Inc.).

Immunohistochemistry

Paraffin sections prepared as described in the previous section were treated with 3% H_2O_2 in Methanol for 30 min in the dark at RT to inactivate endogenous peroxidase. After antigen retrieval, permeabilization and blocking with 10% goat serum (in PBS), the sections were incubated overnight with primary antibodies at 4°C and then incubated for 1 hour at RT with the secondary anti-Rabbit HRP (Boster). The slides were developed using DAB chromogen (Boster) according to the manufacturer's instructions. Nuclei were counterstained with Hematoxylene. Primary antibodies used are: p-Smad 1/5/8 (CST-9511), p-Tak1 (CST-4531), p-p38 (CST-9211) (all from Cell Signaling Technology, 1:50), Scgb1a1 (Abcam, ab40873, 1:750) and α-acetylated

Tubulin (Sigma-Aldrich, T7451, 1:600). Images were captured using Olympus DP72 microscope (Olympus Microsystems).

Quantification of bronchiolar epithelial cells

Lung sections prepared for immunofluorescence microscopy were used to quantify bronchiolar epithelial cells. For each section from one mouse, 8 fields with different terminal bronchioles were selected randomly and imaged. To quantify Scgb1a1^{+} club cells, Scgb1a1^{+} cells and all nuclei (counterstained with DAPI) on bronchiolar epithelium in each field were enumerated using ImageJ, scored as ratio of Scgb1a1^{+} club cells/ total bronchiolar epithelial cells and then averaged to get the final ratio for that mouse. α-Tubulin^{+} ciliated cells and Ki67^{+} proliferating cells were counted in the same way. This procedure was followed for all the genotypes used in this study.

Quantitative Real-Time PCR (qPCR)

Total RNA from lung tissue was extracted with Trizol reagent (Invitrogen, USA) following the manufacturer's instructions. Transcriptor First Strand cDNA synthesis kit (Roche, Basel, Switzerland) with random anchored-oligo (dT) 18 primers and random hexamer was used to synthesize cDNA. qPCR analyses were performed using FS Universal SYBR Green Master Premix (Roche). Reactions were run in triplicate (repeated 3 times independently) in a total volume of 20 µl with Light Cycler 480 Instrument II (Roche). delta-delta Ct (ΔΔCt) method was employed to quantify the relative expression levels of mRNA species. GAPDH (glyceraldehyde 3-phosphate dehydrogenase) served as endogenous control gene to normalize the expression of all

target genes. The primer sequences used for real-time PCR are listed below:

Bmpr1a	F: 5'-TCATGTTCAAGGGCAGAATCTAGA-3'
	R: 5'-GGCAAGGTATCCTCTGGTGCTA-3'
Tak1	F: 5'-CTGCCAGTGAGATGATCG-3'
	R: 5'-CAGGCTCCATACAACTTGAC-3'
Gapdh	F: 5'-CCACAGTCCATGCCATCAC-3'
	R: 5'-CATACCAGGAAATGAGCTTGAC-3'

Western blot analysis

Lung tissue was homogenized in T-PER reagent (Thermo Fisher Scientific) containing added protease and phosphatase inhibitors. Protein concentration was determined using a BCA Protein Assay Kit (Thermo Fisher Scientific). 20 μg of protein lysates of each sample was subjected to SDS-PAGE (8–12%) and transferred onto a nitrocellulose membrane. Immunoblots were then incubated with primary antibodies at 4°C with gentle shaking overnight. After being washed with TBST (Tris-buffered saline, 0.1% Tween 20) three times for 15 min each, blots were incubated with horseradish peroxidase (HRP)-conjugated secondary antibody (Sigma) for 1 hour. Next, the membrane was developed with Super Signal West Femto Maximum Sensitivity Substrate (Thermo Fisher Scientific) and visualized by FluorChem E system (Protein Simple, CA, USA). The following antibodies were used: p-Smad 1/5/8 (CST-9511), Smad 1 (CST-9743), p-Tak1 (CST-4531), Tak1

(CST-4505), p-p38 (CST-9211), p38 (CST-9212) (all from Cell Signaling Technology, 1:1000) and β-Actin (Santa Cruz, Sc-47778, 1:1000).

Statistical analyses

Results were expressed as means ±SD. Comparisons between wild-type and transgenic mice were analyzed using two-tailed unpaired Student's t-test and a *p* value of less than 0.05 was considered to indicate statistical significance (*$p < 0.05$, **$p < 0.01$ and ***$p < 0.001$ when mutant mice were compared with control mice). Each experiment was repeated 3-4 times independently using materials from different mice to confirm the reproducibility of the experimental findings.

Results

Prrx1 marked club cells during development and regeneration

Prrx1 is a marker for mesodermal lateral plate and a transgenic *Prrx1-Cre* mouse line has been generated to label both osteoblast and chondrocytes during bone development [37-39]. Intriguingly, we found that in *Prrx1-Cre; Rosa-tdTomato* mice, tdTomato (tdTO) also labels lung cells. Immunostaining for cell-specific markers on lung sections of two-month-old *Prrx1-Cre; Rosa-tdTomato* mice revealed that tdTomato labeled most club cells (Scgb1a1$^+$), most ciliated cells (α-acetylated Tubulin$^+$, hereinafter referred to as α-Tubulin), and very few fibroblasts (PDGFRα$^+$) (Figure 1A and data not shown). Earlier studies reported that *Prrx1*$^{-/-}$ newborns died from respiratory distress [40, 41]. Since Prrx1 mainly marks club cells in the bronchioles, there is a likelihood that respiratory distress observed in *Prrx1*$^{-/-}$ newborns may have contributions from the bronchioles.

To examine the behavior of Prrx1 lineage cells during bronchiole regeneration and repair, we adopted a Naphthalene (NA)-induced lung injury model. NA is metabolized by CYP-2F2, which is exclusively expressed in club cells, generating cytotoxic epoxide which kills most of the club cells within 1.5 days. Hyperplastic growth occurs at day 3 and the bronchiolar epithelium recovers at day 7 [42]. We exposed the *Prrx1-Cre; Rosa-tdTomato* mice to one dose of NA and the mice were euthanized 3 or 7 days later (Figure 1B). Immunostaining indicated that regenerating club cells (Scgb1a1$^+$) were tdTomato positive at day 3 or 7 (Figures 1C and 1D), suggesting that the Prrx1$^+$ lineage cells also participate in bronchiole

regeneration/repair.

Prrx1 could mark club cells in adult mice

We further traced the Prrx1 lineage cells in adult mice using a tamoxifen (TAM)-inducible *Prrx1-CreERT* mouse line [35]. TAM was injected into 2-month-old *Prrx1-CreERT; Rosa-tdTomato* mice with a total of 3 doses. The mice were euthanized 1 month after the last TAM injection (Figure 1E). Immunostaining results showed that Prrx1 labelled most of the Scgb1a1$^+$ club cells and α-Tubulin$^+$ ciliated cells (Figure 1F), suggesting that *Prrx1-CreERT* mouse can be used to transiently label club and ciliated cells in adult mice. Overall, these findings prove that Prrx1 is expressed by the club cells in adult lungs.

The BMP-Tak1-p38MAPK pathway was activated in bronchiolar cells

BMP signaling pathways are well-established regulators of lung development and lung regeneration/repair mediated by basal cells and AEC2 [31, 32]. A previous study has reported that BMP-Smad1 signaling is activated in club cells in response to NA-induced lung injury [43]. We found that the Tak1-MAPKs pathway was active in bronchiolar epithelial cells under homeostatic conditions as demonstrated by immunohistochemistry (Figure S1A). To determine whether this pathway is also activated during repair/regeneration, we exposed C57BL6 mice to NA and harvested lungs after 3 or 7 days. Immunohistochemistry revealed that Tak1 and p38MAPKs were also activated in the bronchiolar epithelium at both time points after NA exposure (Figure S1A). The levels of p-Tak1 and p-p38 showed considerable increase

at day 3 after NA injury. At day 7, when the repair of bronchiolar epithelium is thought to reach completion, their levels decreased. Overall, these results suggest that the non-canonical BMP pathway is activated in bronchiolar epithelial cells under homeostatic conditions and during regeneration.

Bmpr1a deletion in Prrx1$^+$ cells caused minor defects in bronchiolar homeostasis

To evaluate the functions of BMP signaling pathway in maintenance of bronchiolar epithelium, we generated *Prrx1-CreERT; Bmpr1a$^{f/f}$* mice since deletion of *Bmpr1a* with *Prrx1-Cre* led to embryonic lethality (data not shown). Three doses of TAM were administered intraperitoneally to 2-month-old *Prrx1-CreERT; Bmpr1a$^{f/f}$* and *Bmpr1a$^{f/f}$* mice. The mice were euthanized 2 months later and the lungs were harvested and analyzed (Figure 2A). Quantitative RT-PCR analysis of lungs revealed a significant loss of *Bmpr1a* mRNA in the mutant mice (Figure 2B). Western blot also confirmed a marked decrease in the level of p-Smad 1/5/8 as well as p-Tak1 and p-p38MAPKs in lung samples of the mutant mice (Figure 2C). These results indicate that activation of Tak1-p38Mapk pathway, which are often affected by multiple signaling pathways, are largely controlled by BMPs in bronchiolar epithelial cells. In addition, it appeared that three doses of TAM successfully induced the deletion of *Bmpr1a*. In comparison to the control littermates, the *Prrx1-CreERT; Bmpr1a$^{f/f}$* mice displayed a moderate increase in the numbers of Scgb1a1$^+$ club cells but no significant change in the number of ciliated cells (Figures 2D-G), suggesting that ablation of *Bmpr1a* had modest effect on the homeostasis of adult bronchiolar epithelium. This is in contrast to the critical roles BMPR1A played in lung development since ablating *Bmpr1a* has been shown to disrupt branching morphogenesis and airway formation in the lung and cause neonatal respiratory distress [4, 19, 44]. In addition, *Bmpr1a* ablation in the epithelium by *Sftpc-Cre* resulted in defective lung development, accompanied by reduction in epithelium

proliferation and increased apoptosis [4].

Bmpr1a ablation disrupted club cell regeneration

We then examined the effect of *Bmpr1a* deletion on regeneration of bronchiolar epithelium. Adult *Prrx1-CreERT; Bmpr1a*$^{f/f}$ and control mice were given a single dose of NA following 3 doses of TAM administration. Lungs were harvested 3 or 7 days after NA exposure and processed for immunostaining (Figure 3A). We found that deletion of *Bmpr1a* impaired the repair of bronchiolar epithelium at both time points. Three days after NA exposure, the number of Scgb1a1^{+} club cells present on the bronchioles was significantly reduced in the knockout mice (Figures S2A-C). This was likely due to impaired proliferation of the club cells since terminal bronchioles of *Bmpr1a* ablated mice contained fewer Ki67^{+} proliferative cells than those of control mice (Figures S2B and S2D). The defects in bronchiolar epithelium repair became more prominent at day 7 after NA exposure in the mutant mice, as manifested by decreased numbers of Scgb1a1^{+} club cells and Ki67^{+} cells (Figures 3B-E). However, we did not detect any notable changes in the number of ciliated cells either 3 days (Figures S2B and S2E) or 7 days after NA treatment (Figures 3C and 3F). These results indicate that BMPR1A is crucial for club cell regeneration.

Tak1 deletion in Prrx1^{+} cells led to defective bronchiole and neonatal lethality

We then tested the physiological functions of *Tak1* in lung development using *Prrx1-Cre; Tak1* mice since Tak1 was shown to be activated in bronchiolar epithelial cells during homeostasis in a BMPR1A-dependent manner (Figure S1A and 2C). We found that *Prrx1-Cre; Tak1*$^{f/f}$ pups died shortly after birth. Histological analysis

revealed some anatomical abnormalities in the lungs of knockout pups (Figure 4A). When H/E stained lung sections were examined, we found that the knockout mouse lung was morphologically different from the control. The bronchiolar and alveolar areas were not well differentiated in the knockout mice compared to those of control mice (Figure 4B, left panel). H/E staining also showed that the bronchioles in the knockout mice were poorly organized (Figure 4B, right panel). Immunohistochemistry staining confirmed that Scgb1a1$^+$ club cells and α-Tubulin$^+$ ciliated cells were less differentiated in the mutant mice (Figure 4C-D). To our understanding, development of the bronchiolar epithelium in *Prrx1-Cre; Tak1$^{f/f}$* newborn pups were delayed compared to the control littermates. These results, for the first time, show that *Tak1* is required for the development of bronchiolar epithelium.

Ablation of *Tak1* disrupted club cell regeneration

To determine the functions of *Tak1* in Prrx1$^+$ cells in adult mice, we generated *Prrx1-CreERT; Tak1$^{f/f}$* mice. Three doses of TAM were administered to 2-month-old *Prrx1-CreERT; Tak1$^{f/f}$* and *Tak1$^{f/f}$* mice. Two months later, the mice were euthanized and the lungs were harvested for analyses (Figure 5A). Quantitative RT-PCR revealed a significant loss of *Tak1* mRNA in the mutant mice compared to control littermates (Figure 5B). Depletion of *Tak1* led to a modest decrease in number of Scgb1a1$^+$ club cells and a modest increase in the number α-Tubulin$^+$ ciliated cells (Figures 5C-F).

Next, following TAM administration the *Prrx1-CreERT; Tak1$^{f/f}$* and control mice were exposed to NA and lungs were harvested 3 and 7 days later (Figure 6A).

Three days after NA-induced injury, we observed a significant delay in regeneration of the bronchiolar epithelium as the numbers of Scgb1a1$^+$ club cells and Ki67$^+$ proliferating cells were significantly decreased in the knockout mice (Figures S3A-D), while the number of ciliated cells was barely changed (Figure S3B and S3E). Seven days after NA injury, club cell regeneration and proliferation were more severely affected in *Tak1* deficient mice (Figures 6B-E). However, no detectable effects on the number of ciliated cells was observed (Figures 6C and 6F). These findings indicate that *Tak1* plays an important role in the Prrx1$^+$ cells-mediated regeneration and repair of bronchiolar epithelium, similar to BMPR1A.

Mapk14 deletion in Prrx1$^+$ cells resulted in defects in regeneration

p38MAPKs are important downstream kinases of *Tak1* and are involved in lung epithelial branching morphogenesis [26, 45]. Previous studies have shown that *Mapk14*, the dominant isoform of p38MAPKs in the lung, plays critical roles in lung stem cells and lung development [28]. Indeed, immunohistochemistry revealed that the levels of activated p38 were reduced in *Tak1* knockout mice after NA exposure (Figure 6G). Western blot analysis confirmed decreased levels of p-p38 in the lung tissues of *Tak1* knockout mice 3 days and 7 days after NA administration (Figure 6H-I). The modest decease in p-p38 is likely caused by presence of cells not labelled by Prrx1 in the lung. We then generated *Prrx1-Cre; Mapk14$^{f/f}$* mice to determine the functions of *Mapk14* in club cells in adult mice. Adult *Prrx1-Cre; Mapk14$^{f/f}$* mice have normal appearance. Lungs were harvested from the 2.5-month-old mice and analyzed. We found that ablation of *Mapk14* in Prrx1$^+$ cells resulted in a modest

increase in the number of Scgb1a1^{+} club cells while the number of ciliated cells was not affected (Figure 7A-D). These results indicate that Mapk14 plays minimal roles in the development and homeostasis of bronchiolar epithelia.

To determine the functions of *Mapk14* in regeneration of bronchiolar epithelial cells, we exposed *Prrx1-Cre; Mapk14$^{f/f}$* mice to NA and lungs were harvested 3 and 7 days later (Figure 7E). We observed a significant impairment in regeneration/repair of bronchiolar epithelium at day 3 or 7 after NA exposure in the *Mapk14* ablated mice (Figure S4A and Figure7F). At both time points, the numbers of Scgb1a1^{+} club cells and Ki67^{+} proliferating cells were decreased in the knockout mice (Figures 7G-I and Figures S4B-D) while no significant change in the number of ciliated cells was observed either 3 days (Figures S4B and S4E) or 7 days (Figures 7G and 7J) after NA injury. These findings suggest that *Mapk14* plays important roles in Prrx1 lineage cell-mediated bronchiole regeneration/repair.

Discussion

Our lineage tracing experiments based on transgenic *Prrx1-Cre* and *Prrx1-CreERT* mice lines show that Prrx1 marks club cells and moreover, these club cells can replenish the bronchiolar epithelium during repair, indicating that $Prrx1^+$ club cells act as transiently amplifying progenitor cells. This is a surprising finding as Prrx1 is generally believed to be marker for mesenchymal stem cells, which form bone and cartilage in vivo and can differentiate into osteoblasts, chondrocytes, and adipocytes but not epithelial cells in vitro [46, 47]. Yet the club cells are epithelial cells in nature and are supposed to be derived from the endoderm. During embryonic development, the primary lung bud is surrounded by ventral mesenchyme, which secretes multiple growth regulators such as Wnt and BMP molecules to direct endodermal cell proliferation and differentiation [16, 48]. One possible explanation is that progenitors of club cells are derived from mesenchymal cells via a process termed mesenchymal-epithelial-transition. Another possibility is that Prrx1, the homeobox transcription factor, may play an important role in maintaining the stemness of multiple cell lineages including mesenchymal cells and club cells. A similar example is Lgr5, which is established as a stem cell marker for gastrointestinal epithelial cells but has recently been reported to mark lung fibroblasts [49]. Similarly, club cells are a population of progenitor cells comprising of highly heterogenous subsets. Besides Scgb1a1, club cells marked by Upk3a or Id2 have been reported [8, 50]. While Prrx1 lineage cells do express Scgb1a1 during homeostasis and regeneration, further investigation is needed to examine the relationships among Prrx1

lineage cells and Upk3a-expressing club cells and Id2-marked multipotent club cell progenitors.

BMPs play vital roles in lung development and homeostasis. These factors are supplied by mesenchymal cells and they regulate both cell proliferation and differentiation of lung epithelial cells. As such, disruption of BMP-Smad1 signaling impairs lung development [19, 21, 22]. Moreover, BMPs have been shown to play important roles in lung repair mediated by basal cells and AEC2. The major function of BMPs appears to inhibit cell proliferation in steady-state condition. Up-regulation of BMP inhibitors during injury may promote proliferation of basal cells, AEC2 cells and thus, facilitates the repair process [31, 32]. However, here we show that ablation of *Bmpr1a* resulted in defective regeneration of bronchiolar epithelium. In particular, club cell proliferation and expansion are suppressed in the absence of *Bmpr1a*. Thus, BMPR1A appears to play opposing roles in regeneration of club cells and basal cells and AEC2 [32]. On the other hand, repair of adult lung epithelia is reminiscent of the lung developmental process, and from our results it is evident that, ablation of *Bmpr1a* affects these two processes in a similar fashion. Loss of BMP signaling causes developmental defects associated with impaired epithelial proliferation. For example, inactivation of *Bmpr1a* and *Bmpr1b* results in tracheal agenesis [16] and *Bmpr1a* ablation in lung epithelial cells resulted in defective lung development, accompanied by reduction in epithelial proliferation and extensive apoptosis [4].

Moreover, the effects of *Bmpr1a* ablation on bronchiolar epithelium regeneration are reproduced by ablation of *Tak1* or *Mapk14*, which are activated in

club cells in a BMPR1A-dependent manner. While *Tak1* is known to promote cell proliferation and survival [51, 52], activation of p38MAPKs often inhibits cell proliferation, in particular after activation by stress and cytokines [53]. Indeed, it has been reported that p38MAPKs promote the differentiation but inhibits the proliferation of lung stem cells in a mouse model in which *Mapk14* was deleted using a *CreERT* driven by RERTn, which encodes the large subunit of RNA polymerase II [28]. On the other hand, there are examples where p38MPAKs have been shown to promote cell proliferation [54, 55]. A recent study also reported that Notch1 is required for club cell regeneration [56]. Since Notch1 signaling crosstalks with p38MAPKs [57, 58], future studies will be needed to test their functional link in club cell regeneration. Nevertheless, our genetic evidence indicates that both Tak1 and p38MAPKs play positive roles in club cell proliferation and expansion during regeneration.

The present study also sheds light on the function of the Tak1-p38MAPK pathway in lung development. We found that *Tak1* deletion in Prrx1-expressing cells led to delayed development of bronchiolar epithelium with the mice dying right after birth. However, we found that ablation of *Mapk14* from $Prrx1^{+}$ lineage cells did not cause obvious phenotypes in the bronchiolar epithelium. This is in contrast with previous studies showing that *Mapk14* is essential for lung development, especially in lung stem cells [28]. One possible explanation is that the same signal may have different effects on stem/progenitor cells located at different sites of the airways, which certainly warrants further investigation.

Conclusion

Our genetic lineage tracing and gene knockout studies indicate that club cells in bronchiole can be marked by homeobox transcription factor Prrx1. Moreover, the BMPR1A-Tak1-p38MAPK pathway plays critical roles in club cell regeneration. Since club cells constitute about 70% of cells in the terminal bronchiolar epithelium, which is also a major site for development of various lung diseases, our study identifies BMPR1A-Tak1-p38MAPK pathway as a potential clinical target to treat bronchiole-related disorders.

Acknowledgements

The work was supported by the National Key Scientific Program (2017YFA0103602 and 2018YFA0800803), National Natural Science Foundation of China (81130039 and 81421061) and also by the Grants from the State Key Laboratory of Oncogenes and Related Genes No. 90-17-03.

Author Contributions

M.S.: Conception and design, Conducting experiments, Collection and/or assembly of data, Data analysis and interpretation, Manuscript writing, Manuscript revision; S.B.: Conducting experiments, Collection and/or assembly of data, Manuscript revision; P.L.: Conducting experiments; Y.M.: Provision of study material; B.L.: Conception and design, Financial support, Data analysis and interpretation, Manuscript writing, Manuscript revision, Final approval of manuscript; H.L.: Conception and design, Manuscript revision, Final approval of manuscript.

Disclosure of Potential Conflicts of Interest

The authors indicated no potential conflicts of interest.

Data Availability

Data supporting the findings of this study are included within the article and available upon request to the corresponding author (liuhj@sjtu.edu.cn).

References

1 Herriges, M. and E.E. Morrisey, Lung development: orchestrating the generation and regeneration of a complex organ. Development, 2014. **141**(3): p. 502-513.

2 Hogan, B.L., et al., Repair and regeneration of the respiratory system: complexity, plasticity, and mechanisms of lung stem cell function. Cell Stem Cell, 2014. **15**(2): p. 123-138.

3 Metzger, R.J., et al., The branching programme of mouse lung development. Nature, 2008. **453**(7196): p. 745-750.

4 Eblaghie, M.C., et al., Evidence that autocrine signaling through Bmpr1a regulates the proliferation, survival and morphogenetic behavior of distal lung epithelial cells. Dev Biol, 2006. **291**(1): p. 67-82.

5 Rock, J.R., et al., Notch-dependent differentiation of adult airway basal stem cells. Cell Stem Cell, 2011. **8**(6): p. 639-648.

6 Guha, A., et al., Neuroepithelial body microenvironment is a niche for a distinct subset of Clara-like precursors in the developing airways. Proc Natl Acad Sci USA, 2012. **109**(31): p. 12592-12597.

7 Kumar, P.A., et al., Distal airway stem cells yield alveoli in vitro and during lung regeneration following H1N1 influenza infection. Cell, 2011. **147**(3): p. 525-538.

8 Rawlins, E.L., et al., The role of Scgb1a1+ Clara cells in the long-term maintenance and repair of lung airway, but not alveolar, epithelium. Cell Stem Cell, 2009. **4**(6): p. 525-534.

9 Reynolds, S.D., et al., Conditional clara cell ablation reveals a self-renewing progenitor function of pulmonary neuroendocrine cells. Am J Physiol Lung Cell Mol Physiol, 2000. **278**(6): p. L1256-1263.

10 Tata, P.R., et al., Dedifferentiation of committed epithelial cells into stem cells in vivo. Nature, 2013. **503**(7475): p. 218-223.

11 Watson, J.K., et al., Clonal Dynamics Reveal Two Distinct Populations of Basal Cells in Slow-Turnover Airway Epithelium. Cell Rep, 2015. **12**(1): p. 90-101.

12 Guha, A., et al., Uroplakin 3a(+) Cells Are a Distinctive Population of Epithelial Progenitors that Contribute to Airway Maintenance and Post-injury Repair. Cell Rep, 2017. **19**(2): p. 246-254.

13 Green, M.D., et al., Stem cells of the respiratory system: from identification to differentiation into

functional epithelium. Bioessays, 2013. **35**(3): p. 261-270.

14 Kajstura, J., et al., Evidence for human lung stem cells. N Engl J Med, 2011. **364**(19): p. 1795-1806.

15 Bellusci, S., et al., Evidence from normal expression and targeted misexpression that bone morphogenetic protein (Bmp-4) plays a role in mouse embryonic lung morphogenesis. Development, 1996. **122**(6): p. 1693-1702.

16 Domyan, E.T., et al., Signaling through BMP receptors promotes respiratory identity in the foregut via repression of Sox2. Development, 2011. **138**(5): p. 971-981.

17 Geng, Y., et al., Follistatin-like 1 (Fstl1) is a bone morphogenetic protein (BMP) 4 signaling antagonist in controlling mouse lung development. Proc Natl Acad Sci USA, 2011. **108**(17): p. 7058-7063.

18 Li, Q., et al., Histone arginine methylation by Prmt5 is required for lung branching morphogenesis through repression of BMP signaling. J Cell Sci, 2018. **131**(14).

19 Weaver, M., et al., Bmp signaling regulates proximal-distal differentiation of endoderm in mouse lung development. Development, 1999. **126**(18): p. 4005-4015.

20 Heldin, C.H., et al., TGF-beta signalling from cell membrane to nucleus through SMAD proteins. Nature, 1997. **390**(6659): p. 465-471.

21 Chen, C., et al., Smad1 expression and function during mouse embryonic lung branching morphogenesis. Am J Physiol Lung Cell Mol Physiol, 2005. **288**(6): p. L1033-1039.

22 Xu, B., et al., Smad1 and its target gene Wif1 coordinate BMP and Wnt signaling activities to regulate fetal lung development. Development, 2011. **138**(5): p. 925-935.

23 Kua, H.Y., et al., c-Abl promotes osteoblast expansion by differentially regulating canonical and non-canonical BMP pathways and p16INK4a expression. Nat Cell Biol, 2012. **14**(7): p. 727-737.

24 Shibuya, H., et al., Role of TAK1 and TAB1 in BMP signaling in early Xenopus development. EMBO J, 1998. **17**(4): p. 1019-1028.

25 Shim, J.H., et al., TAK1 is an essential regulator of BMP signalling in cartilage. EMBO J, 2009. **28**(14): p. 2028-2041.

26 Liu, Y., et al., Role for mitogen-activated protein kinase p38 alpha in lung epithelial branching

morphogenesis. Dev Biol, 2008. **314**(1): p. 224-235.

27 Hui, L., et al., p38alpha suppresses normal and cancer cell proliferation by antagonizing the JNK-c-Jun pathway. Nat Genet, 2007. **39**(6): p. 741-749.

28 Ventura, J.J., et al., p38alpha MAP kinase is essential in lung stem and progenitor cell proliferation and differentiation. Nat Genet, 2007. **39**(6): p. 750-758.

29 Myllarniemi, M., et al., Gremlin-mediated decrease in bone morphogenetic protein signaling promotes pulmonary fibrosis. Am J Respir Crit Care Med, 2008. **177**(3): p. 321-329.

30 Rosendahl, A., et al., Activation of bone morphogenetic protein/Smad signaling in bronchial epithelial cells during airway inflammation. Am J Respir Cell Mol Biol, 2002. **27**(2): p. 160-169.

31 Tadokoro, T., et al., BMP signaling and cellular dynamics during regeneration of airway epithelium from basal progenitors. Development, 2016. **143**(5): p. 764-773.

32 Chung, M.I., et al., Niche-mediated BMP/SMAD signaling regulates lung alveolar stem cell proliferation and differentiation. Development, 2018. **145**(9).

33 Barnes, P.J., Senescence in COPD and Its Comorbidities. Annu Rev Physiol, 2017. **79**: p. 517-539.

34 Sutherland, K.D. and A. Berns, Cell of origin of lung cancer. Mol Oncol, 2010. **4**(5): p. 397-403.

35 Kawanami, A., et al., Mice expressing GFP and CreER in osteochondro progenitor cells in the periosteum. Biochem Biophys Res Commun, 2009. **386**(3): p. 477-482.

36 Mishina, Y., et al., Generation of Bmpr/Alk3 conditional knockout mice. Genesis, 2002. **32**(2): p. 69-72.

37 Li, P., et al., Roles for HB-EGF in Mesenchymal Stromal Cell Proliferation and Differentiation During Skeletal Growth. J Bone Miner Res, 2019. **34**(2): p. 295-309.

38 Logan, M., et al., Expression of Cre Recombinase in the developing mouse limb bud driven by a Prxl enhancer. Genesis, 2002. **33**(2): p. 77-80.

39 Wu, H., et al., Bone Size and Quality Regulation: Concerted Actions of mTOR in Mesenchymal Stromal Cells and Osteoclasts. Stem Cell Reports, 2017. **8**(6): p. 1600-1616.

40 Ihida-Stansbury, K., et al., Paired-related homeobox gene Prx1 is required for pulmonary vascular development. Circ Res, 2004. **94**(11): p. 1507-1514.

41 Martin, J.F., et al., The paired-like homeo box gene MHox is required for early events of skeletogenesis in multiple lineages. Genes Dev, 1995. **9**(10): p. 1237-1249.

42 Hong, K.U., et al., Clara cell secretory protein-expressing cells of the airway neuroepithelial body microenvironment include a label-retaining subset and are critical for epithelial renewal after progenitor cell depletion. Am J Respir Cell Mol Biol, 2001. **24**(6): p. 671-681.

43 Sountoulidis, A., et al., Activation of the canonical bone morphogenetic protein (BMP) pathway during lung morphogenesis and adult lung tissue repair. PLoS One, 2012. **7**(8): p. e41460.

44 Sun, J., et al., Prenatal lung epithelial cell-specific abrogation of Alk3-bone morphogenetic protein signaling causes neonatal respiratory distress by disrupting distal airway formation. Am J Pathol, 2008. **172**(3): p. 571-582.

45 Wu, X., et al., Ubiquitin-conjugating enzyme Ubc13 controls breast cancer metastasis through a TAK1-p38 MAP kinase cascade. Proc Natl Acad Sci USA, 2014. **111**(38): p. 13870-13875.

46 Biswas, S., et al., BMPRIA is required for osteogenic differentiation and RANKL expression in adult bone marrow mesenchymal stromal cells. Sci Rep, 2018. **8**(1): p. 8475.

47 Cong, Q., et al., p38alpha MAPK Regulates Lineage Commitment and OPG Synthesis of Bone Marrow Stromal Cells to Prevent Bone Loss under Physiological and Pathological Conditions. Stem Cell Reports, 2016. **6**(4): p. 566-578.

48 Que, J., et al., Multiple dose-dependent roles for Sox2 in the patterning and differentiation of anterior foregut endoderm. Development, 2007. **134**(13): p. 2521-2531.

49 Lee, J.H., et al., Anatomically and Functionally Distinct Lung Mesenchymal Populations Marked by Lgr5 and Lgr6. Cell, 2017. **170**(6): p. 1149-1163 e1112.

50 Rawlins, E.L., et al., The Id2+ distal tip lung epithelium contains individual multipotent embryonic progenitor cells. Development, 2009. **136**(22): p. 3741-3745.

51 Mihaly, S.R., et al., TAK1 control of cell death. Cell Death Differ, 2014. **21**(11): p. 1667-1676.

52 Ogura, Y., et al., TAK1 modulates satellite stem cell homeostasis and skeletal muscle repair. Nat Commun, 2015. **6**: p. 10123.

53 Oeztuerk-Winder, F. and J.J. Ventura, The many faces of p38 mitogen-activated protein kinase in

progenitor/stem cell differentiation. Biochem J, 2012. **445**(1): p. 1-10.

54 Matsumoto, T., et al., p38 MAP kinase negatively regulates endothelial cell survival, proliferation, and differentiation in FGF-2-stimulated angiogenesis. J Cell Biol, 2002. **156**(1): p. 149-160.

55 Wada, M., et al., P38 delta MAPK promotes breast cancer progression and lung metastasis by enhancing cell proliferation and cell detachment. Oncogene, 2017. **36**(47): p. 6649-6657.

56 Xing, Y., et al., NOTCH1 is required for regeneration of Clara cells during repair of airway injury. Stem Cells, 2012. **30**(5): p. 946-955.

57 Androutsellis-Theotokis, A., et al., Notch signalling regulates stem cell numbers in vitro and in vivo. Nature, 2006. **442**(7104): p. 823-826.

58 Cook, B.D. and T. Evans, BMP signaling balances murine myeloid potential through SMAD-independent p38MAPK and NOTCH pathways. Blood, 2014. **124**(3): p. 393-402.

Figure Legends

Figure 1. Prrx1 labeled club cells in the lung.

(A) Two-month-old *Prrx1-Cre; Rosa-tdTomato* mice were used for in vivo tracing of Prrx1 lineage. Immunostaining was performed on lung sections with Scgb1a1 (top panel) and α-Tubulin (bottom panel) for club cells and ciliated cells, respectively. Nuclei were counterstained with DAPI (blue). Inset, enlarged view of indicated region showing a representative tdTomato^{+} Scgb1a1^{+} club cell. tdTO, tdTomato. Scale bar, 50 μm.

(B) Schedule of naphthalene (NA) administration and tissue collection to *Prrx1-Cre; Rosa-tdTomato* mice. NA was administered through intraperitoneal (i.p) injection and lungs were harvested after 3 or 7 days and then stained with club cell marker Scgb1a1. dpi, day post injury.

(C-D) Regenerating club cells retained the tdTomato labeling (C) 3 day and (D) 7 day after NA treatment, confirming their *Prrx1* lineage. Inset, enlarged view of indicated region. Scale bar, 50 μm.

(E) Schematic of TAM treatment to 2-month-old *Prrx1-CreERT; Rosa-tdTomato* mice.

(F) Immunostaining of Scgb1a1 (top panel) and α-Tubulin (bottom panel) on lung sections of *Prrx1-CreERT; Rosa-tdTomato* mice. Nuclei were counterstained with DAPI. Scale bar, 50 μm.

Figure 2. Depletion of *Bmpr1a* produced minimal effects on homeostatic bronchiolar epithelium.

(A) Schematic of TAM treatment to 2-month-old *Prrx1-CreERT; Bmpr1a*$^{f/f}$ and *Bmpr1a*$^{f/f}$ (control) mice.

(B) Successful deletion of *Bmpr1a* gene after TAM injection was confirmed by qPCR analysis (n = 6 mice for each genotype). **$p<0.01$.

(C) Western blot detected considerable decreases in the levels of p-Smad 1/5/8, p-Tak1 and p-p38 in the *Bmpr1a* deleted lungs compared to the control.

(D) Histological examination of *Bmpr1a* knockout and control lung sections revealed little difference. Scale bar, 50 μm.

(E) Immunostaining of Scgb1a1 (left panel) and α-Tubulin (right panel) on lung sections of mutant and control mice two month after TAM administration. Nuclei were counterstained with DAPI. Scale bar, 50 μm.

(F-G) Quantification of Scgb1a1^{+} cells (F) and α-Tubulin^{+} cells (G) per total

bronchiolar epithelial cells (BECs). For each lung section, 8 different fields were quantified and averaged (n = 6 mice for each genotype). *p<0.05. NS, not significant.

Figure 3. BMPR1A was crucial for club cell regeneration.

(A) Schematic of NA injury and tissue collection following TAM treatment to 2-month-old *Prrx1-CreERT; Bmpr1a*$^{f/f}$ and control mice.

(B) H/E staining of the lung sections of *Prrx1-CreERT; Bmpr1a*$^{f/f}$ and *Bmpr1a*$^{f/f}$ mice 7 days after NA injury revealed bronchiolar structure defects in the mutant mice. Scale bar, 50 μm.

(C) Immunostaining of Scgb1a1 (left panel), Ki67 (middle panel) and α-Tubulin (right panel) 7 days after NA administration. Nuclei were counterstained with DAPI. Scale bar, 50 μm.

(D-F) Quantification of Scgb1a1^{+} cells (D), Ki67^{+} cells (E) and α-Tubulin^{+} cells (F) per total bronchiolar epithelial cells (BECs) 7 days after NA administration. For each lung section, 8 different fields were quantified and averaged (n = 6 mice for each genotype). ***p<0.001. **p<0.01. NS, not significant.

Figure 4. Postnatal lethality with delayed bronchiole development resulted from *Tak1* ablation in *Prrx1*$^+$ cells.

(A) Newborn *Prrx1-Cre; Tak1*$^{f/f}$ mice died shortly after birth. Newborn pups' macrograph.

(B) H/E staining revealed morphological differences in the *Tak1* knockout and control mouse lung sections. Scale bars, 500 μm (left panel) and 50 μm (right panel).

(C) Immunohistochemistry of Scgb1a1 for club cells. Lower magnification is provided on the left panel and higher magnification is on the right panel. Sections were developed using DAB chromogen and nuclei were counterstained with Hematoxylene. Scale bars, 100 μm (left panel) and 20 μm (right panel).

(D) Immunohistochemistry of α-Tubulin for ciliated cells. Lower magnification is provided on the left panel and higher magnification is on the right panel. Sections were developed using DAB chromogen and nuclei were counterstained with Hematoxylene. Scale bars, 100 μm (left panel) and 20 μm (right panel).

Figure 5. *Tak1* ablation in *Prrx1*$^+$ cells resulted in a minor defect in club cell homeostasis.

(A) Schematic of TAM treatment of 2-month-old *Prrx1-CreERT; Tak1*$^{f/f}$ and *Tak1*$^{f/f}$ (control) mice.

(B) qPCR analysis illustrates the successful deletion of *Tak1* gene after TAM administration (n = 6 mice for each genotype). **p<0.01.

(C) H/E staining of *Tak1* knockout and control lung sections after TAM administration. Scale bar, 50 μm.

(D) Immunostaining of Scgb1a1 (left panel) and α-Tubulin (right panel) of *Tak1* ablated and control lung sections after 3 doses of TAM. Nuclei were counterstained with DAPI. Scale bar, 50 μm.

(E-F) Quantification of Scgb1a1$^+$ cells (E) and α-Tubulin$^+$ cells (F) per total bronchiolar epithelial cells. For each lung section, 8 different fields were quantified and averaged (n = 6 mice for each genotype). *p<0.05.

Figure 6. Ablation of *Tak1* in *Prrx1*$^+$ cells resulted in severe defect in club cell regeneration.

(A) Schematic of NA administration and tissue collection following TAM treatment to 2-month-old *Prrx1-CreERT; Tak1$^{f/f}$* and control mice.

(B) H/E staining of the lung sections of *Prrx1-CreERT; Tak1$^{f/f}$* and *Tak1$^{f/f}$* mice 7 days after NA administration revealed bronchiolar structure defects in the mutant mice. Scale bar, 50 μm.

(C) Immunostaining of Scgb1a1 (left panel), Ki67 (middle panel) and α-Tubulin (right panel) on lung sections of *Tak1* knockout and control mice 7 days after NA injury. Nuclei were counterstained with DAPI. Scale bar, 50 μm.

(D-F) Quantification of Scgb1a1$^+$ cells (D), Ki67$^+$ cells (E) and α-Tubulin$^+$ cells (F) per total bronchiolar epithelial cells 7 days following NA exposure. For each lung section, 8 different fields were quantified and averaged (n = 6 mice for each genotype). **p<0.01. ***p<0.001. NS, not significant.

(G) Immunohistochemistry of p-p38MAPKs on lung sections of *Prrx1-CreERT; Tak1$^{f/f}$* and control mice 3 days (left panel) and 7 days (right panel) after NA injury.

Sections were developed using DAB chromogen and nuclei were counterstained with Hematoxylene. Scale bar, 50 μm.

(H-I) Western blot analysis detected significant decreases in the levels of p-p38 in the *Tak1* deficient mouse lung samples compared to the control 3 days (H) or 7 days (I) after NA administration. Left panel: representative western blot result; right panel: quantification of relative protein expressions plotted in the graph as fold change in protein expression (n = 3 mice for each genotype). *p< 0.05. dpi, day post injury.

Figure 7. Deletion of Mapk14 in Prrx1+ cells impaired regeneration of bronchiolar epithelium.

(A) H/E staining of the *Prrx1-Cre; Mapk14$^{f/f}$* and *Mapk14$^{f/f}$* lung sections revealed little difference. Scale bar, 50 μm.

(B) Immunostaining of Scgb1a1 (left panel) and α-Tubulin (right panel). Nuclei were counterstained with DAPI. Scale bar, 50 μm.

(C-D) Quantification of Scgb1a1^{+} cells (C) and α-Tubulin^{+} cells (D) per total bronchiolar epithelial cells (BECs). For each lung section, 8 different fields were quantified and averaged (n = 6 mice for each genotype). *p<0.05. NS, not significant.

(E) Schematic of NA administration and tissue collection to *Prrx1-Cre; Mapk14$^{f/f}$* and control mice.

(F) Histological examination of *Mapk14* knockout and control lung sections 7 days after NA exposure revealed bronchiolar structure defects in the mutant mice. Scale bar, 50 μm.

(G) Immunostaining of Scgb1a1 (left panel), Ki67 (middle panel) and α-Tubulin

(right panel) 7 days after NA injury. Nuclei were counterstained with DAPI. Scale bar, 50 μm.

(H-J) Quantification of Scgb1a1^{+} cells (H), Ki67^{+} cells (I) and α-Tubulin^{+} cells (J) per total bronchiolar epithelial cells 7 days after NA exposure. For each lung section, 8 different fields were quantified and averaged (n = 6 mice for each genotype).

*$p<0.05$. NS, not significant.

Supplemental Figure Legends

Figure S1. The non-canonical BMP pathway is activated in club cells.

(A) Immunohistochemistry revealed the activation of Tak1-P38Mapk signaling in the club cells at steady-state condition as well as 3 and 7 days after NA exposure. Lung sections were stained for p-Tak1 and p-p38 and developed using DAB chromogen. Nuclei were counterstained with Hematoxylene. WT, wild type; dpi, day post injury. Scale bar, 50 μm.

Figure S2. *Prrx1-CreERT; Bmpr1a*$^{f/f}$ shows defects in bronchiolar epithelium repair after NA exposure.

(A) H/E staining of the lung sections of *Prrx1-CreERT; Bmpr1a*$^{f/f}$ and *Bmpr1a*$^{f/f}$ mice 3 days after NA injury. Scale bar, 50 μm.

(B) Immunostaining of Scgb1a1 (left panel), Ki67 (middle panel) and α-Tubulin (right panel) 3 days after NA injury. Nuclei were counterstained with DAPI. Scale bar, 50 μm.

(C-E) Quantification of Scgb1a1^{+} cells (C), Ki67^{+} cells (D) and α-Tubulin^{+} cells (E) per total bronchiolar epithelial cells (BECs) 3 days after NA exposure. For each lung section, 8 different fields were quantified and averaged (n = 6 mice for each genotype). *p<0.05. NS, not significant.

Figure S3. *Tak1* deletion resulted in impaired club cell regeneration.

(A) H/E staining of the lung sections of *Prrx1-CreERT; Tak1*$^{f/f}$ and *Tak1*$^{f/f}$ mice 3 days

after NA injury. Scale bar, 50 μm.

(B) Immunostaining of Scgb1a1 (left panel), Ki67 (middle panel) and α-Tubulin (right panel) on lung section of mutant and control mice 3 days after NA injury. Nuclei were counterstained with DAPI. Scale bar, 50 μm.

(C-E) Quantification of Scgb1a1$^+$ cells (C), Ki67$^+$ cells (D) and α-Tubulin$^+$ cells (E) per total bronchiolar epithelial cells 3 days following NA exposure. For each lung section, 8 different fields were quantified and averaged (n = 6 mice for each genotype). ***p<0.001. **p<0.01. NS, not significant.

Figure S4. Bronchiolar epithelium fails to repair after naphthalene injury due to loss of *Mapk14*.

(A) H/E staining of the lung sections of *Prrx1-Cre; Mapk14$^{f/f}$* and *Mapk14$^{f/f}$* mice 3 days after NA exposure. Scale bar, 50 μm.

(B) Immunostaining of Scgb1a1 (left), Ki67 (middle) and α-Tubulin (right) on lung sections of *Prrx1-Cre; Mapk14$^{f/f}$* and *Mapk14$^{f/f}$* mice 3 days after NA injury. Nuclei were counterstained with DAPI (blue). Scale bar, 50 μm.

(C-E) Quantification of Scgb1a1$^+$ (C), Ki67$^+$ (D) and α-Tubulin$^+$ (E) cells per total bronchiolar epithelial cells 3 days following NA injury. For each lung section, 8 different fields were quantified and averaged (n = 6 mice for each genotype). *p<0.05. NS, not significant.

Legend for Graphical Abstract

Schematic representation of our results showing the critical roles of the non-canonical signaling pathway of BMPs, (BMPR1A-Tak1-p38MAPK) in club cell regeneration. Naphthalene (NA) is metabolized by CYP-2F2, which is expressed exclusively in club cells, generating cytotoxic epoxide that kills the club cells within 1.5 days after NA exposure. Under normal conditions, hyperplastic growth occurs at day 3 and the bronchiolar epithelium is restored at day 7. We show that ablation of *Bmpr1a*, *Tak1*, or *Mapk14* (encoding p38α) in club cells resulted in severe defects in regeneration and bronchiole repair in adult mice.

Figure 1

Huijuan Liu

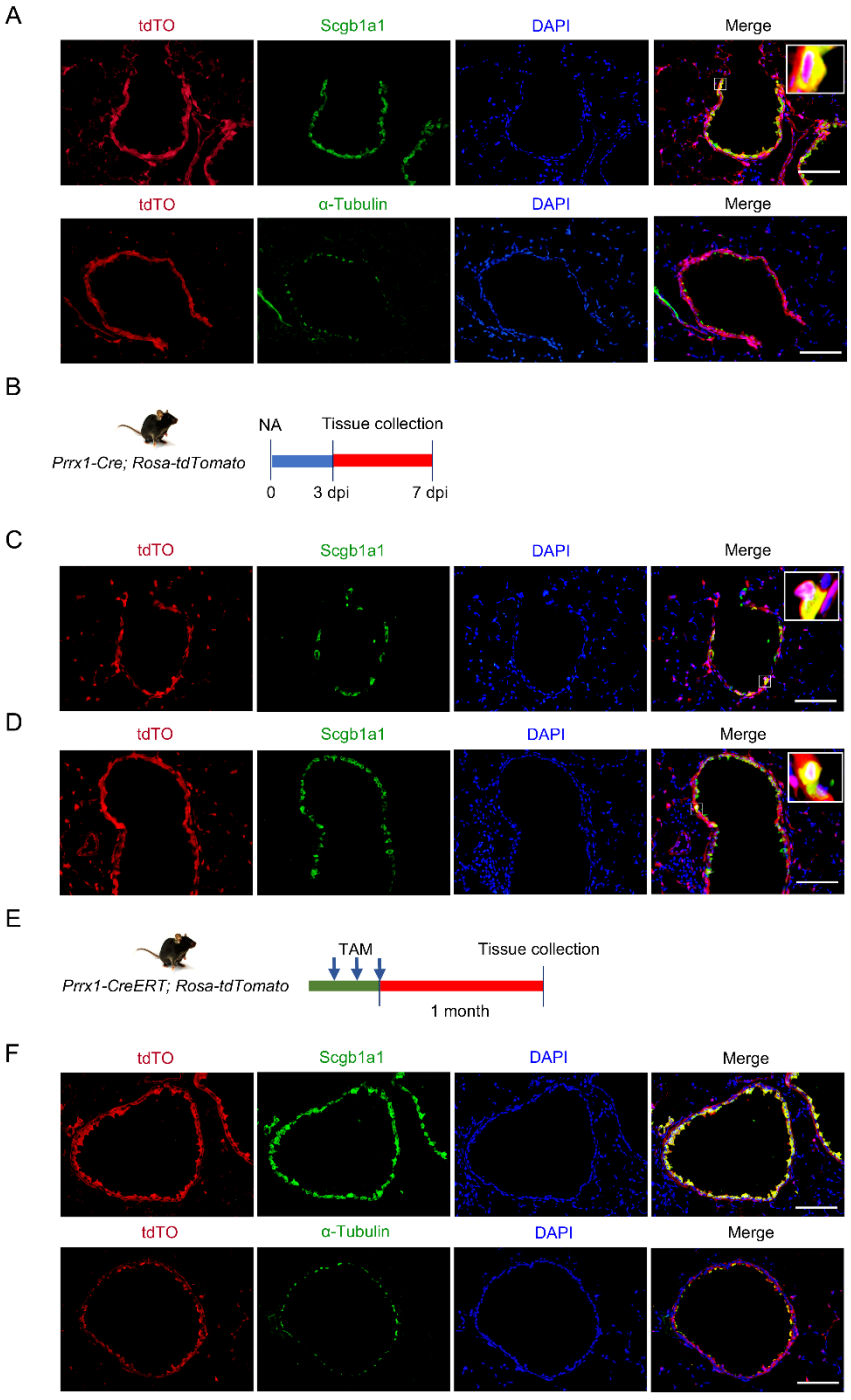

Figure 2

Huijuan Liu

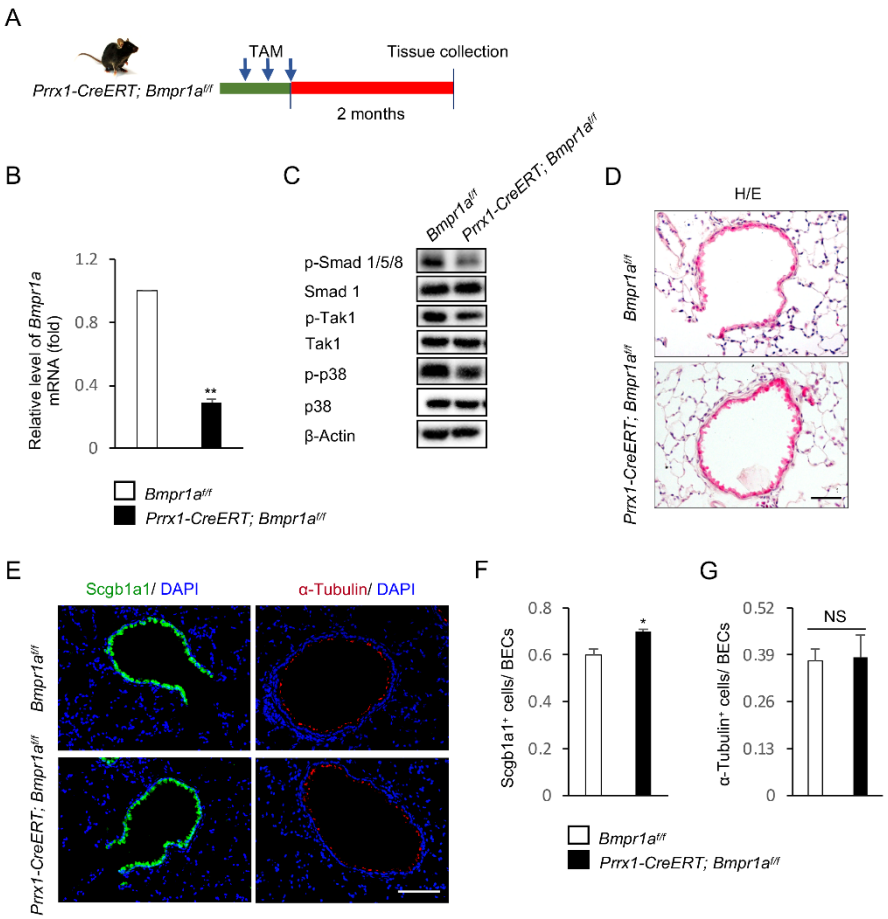

Figure 3 **Huijuan Liu**

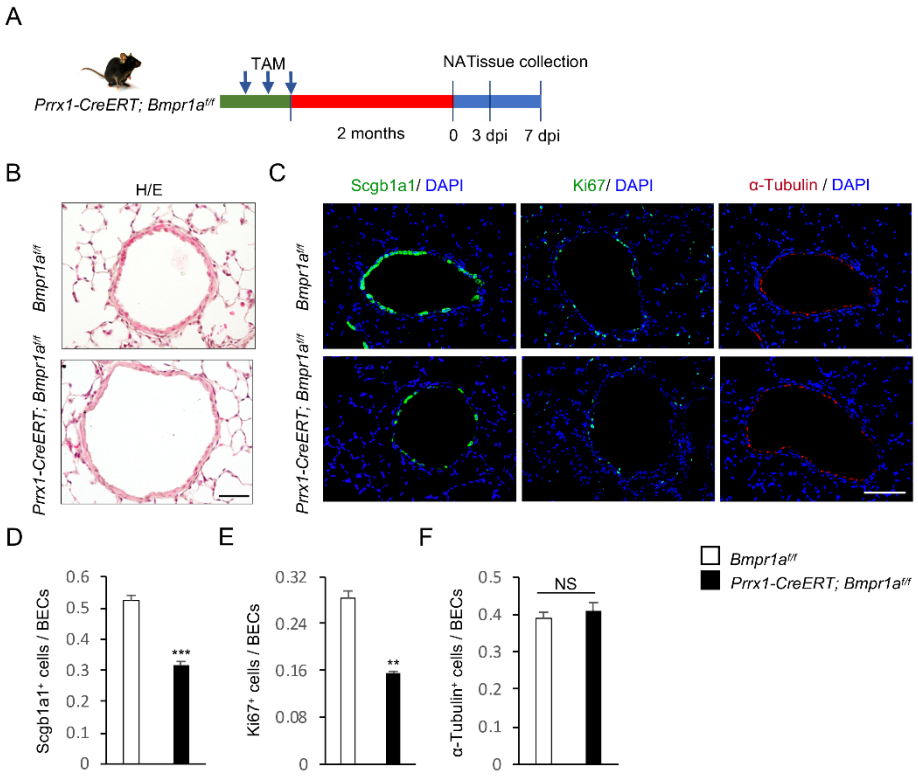

Figure 4

Huijuan Liu

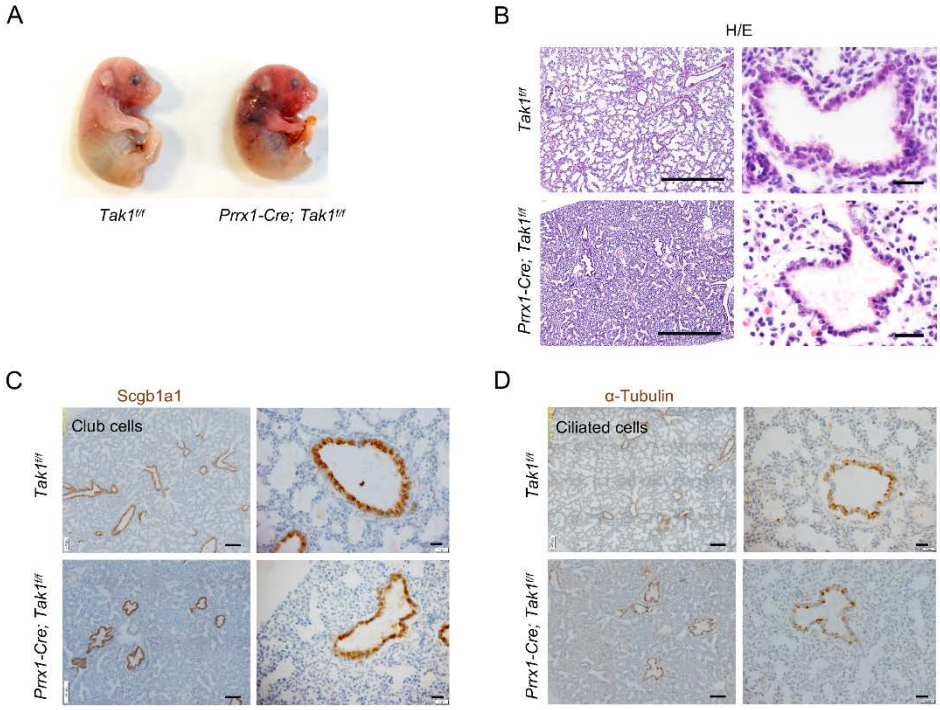

Figure 5

Huijuan Liu

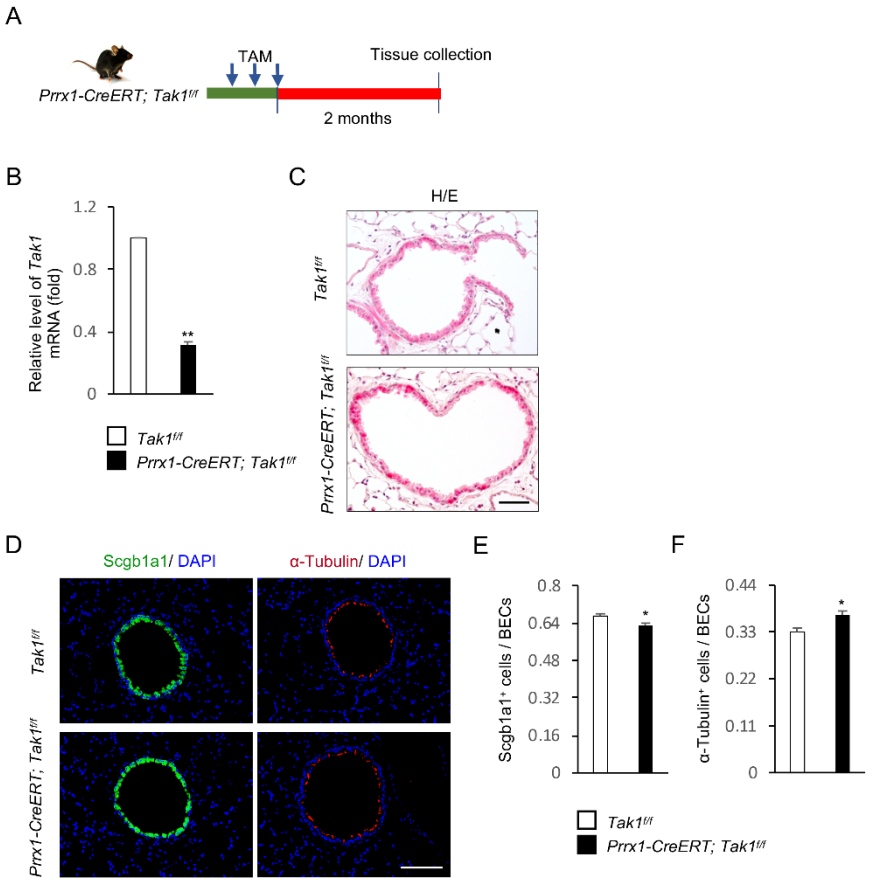

Figure 6 **Huijuan Liu**

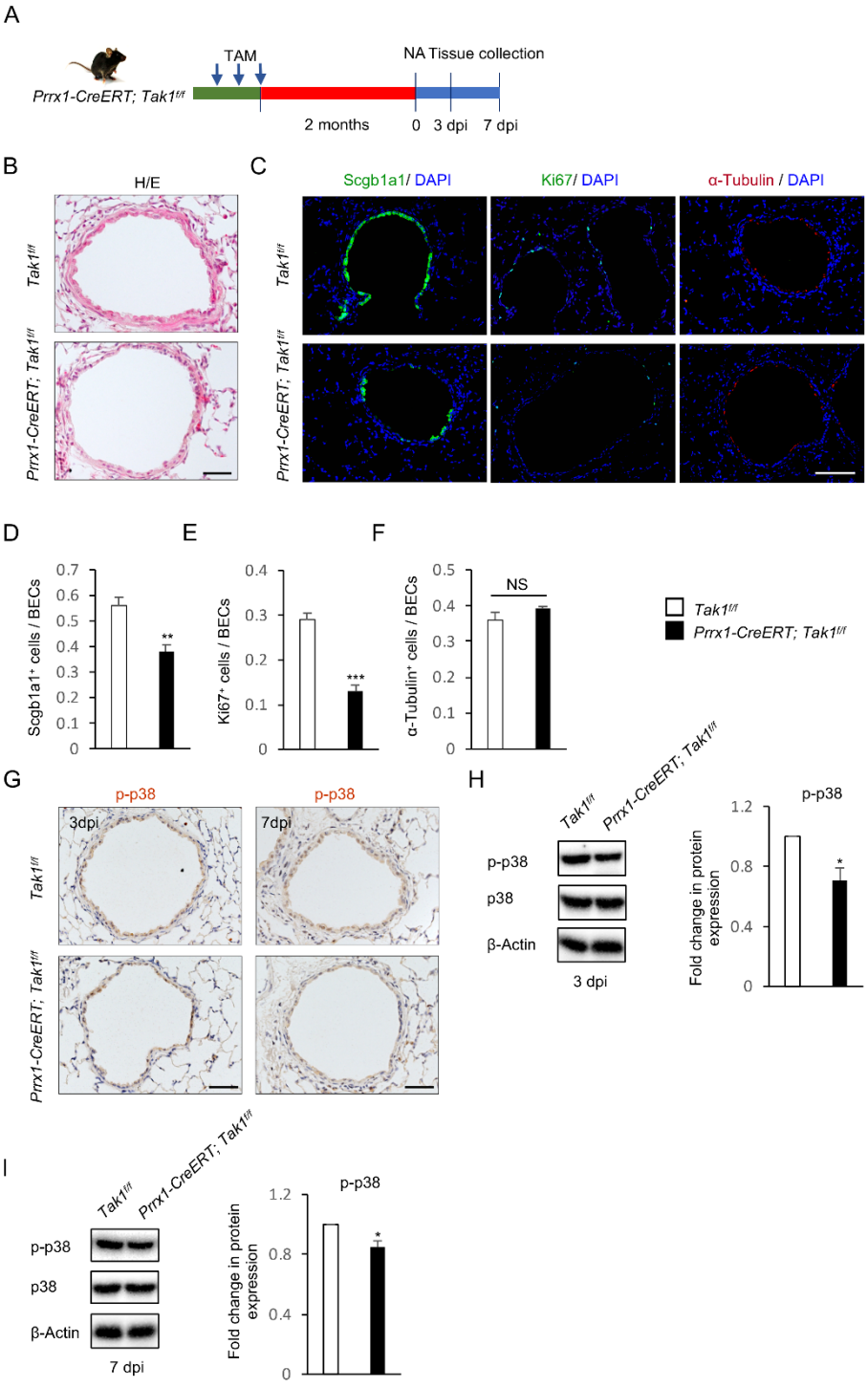

Figure 7

Huijuan Liu

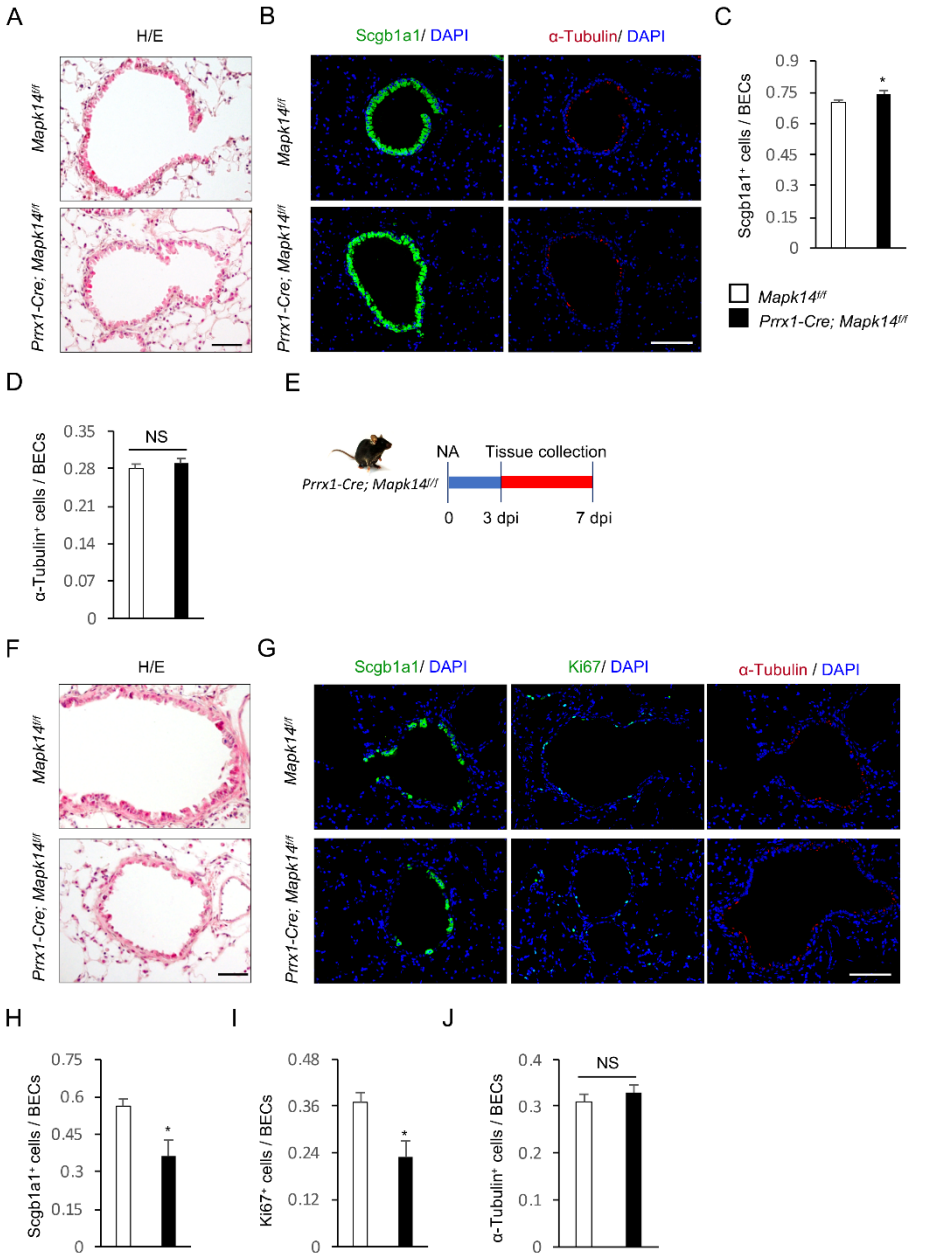

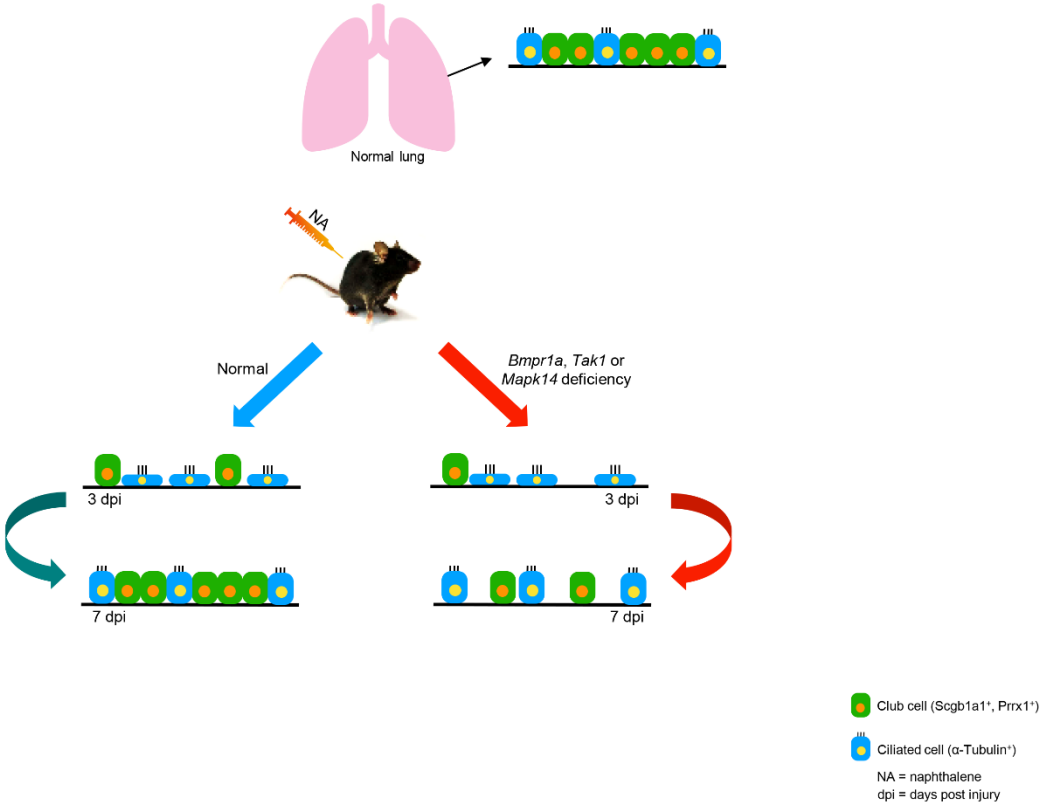

Figure 1 **Huijuan Liu**

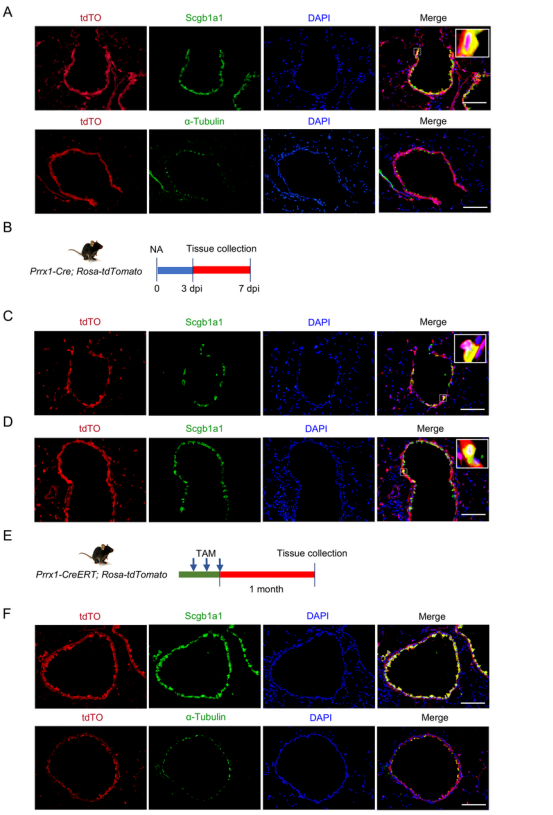

STEM_3125_Figure-1.tif

Figure 2 **Huijuan Liu**

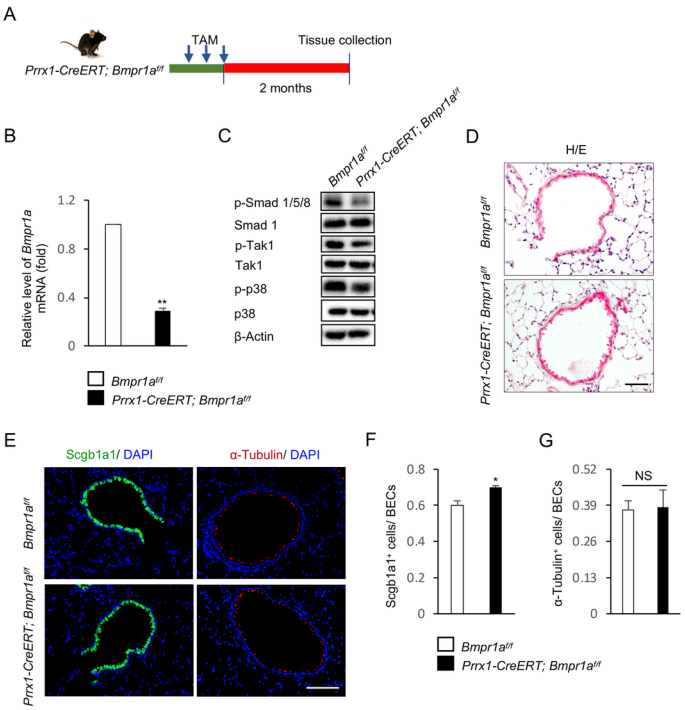

STEM_3125_Figure-2.tif

Figure 3 **Huijuan Liu**

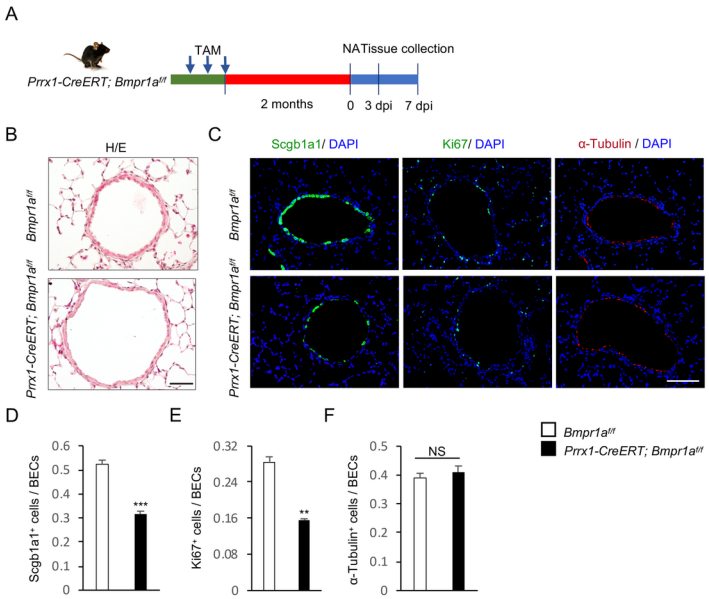

STEM_3125_Figure-3.tif

Figure 4

Huijuan Liu

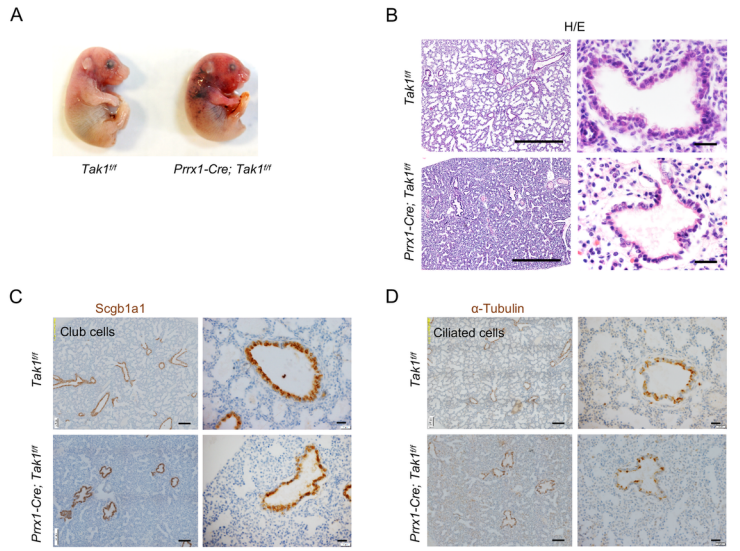

STEM_3125_Figure-4.tif

Figure 5

Huijuan Liu

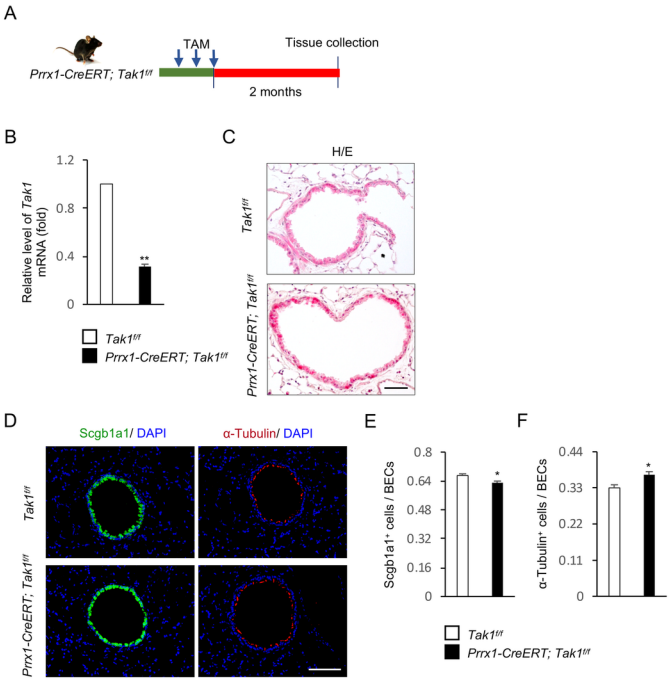

STEM_3125_Figure-5.tif

Figure 6 **Huijuan Liu**

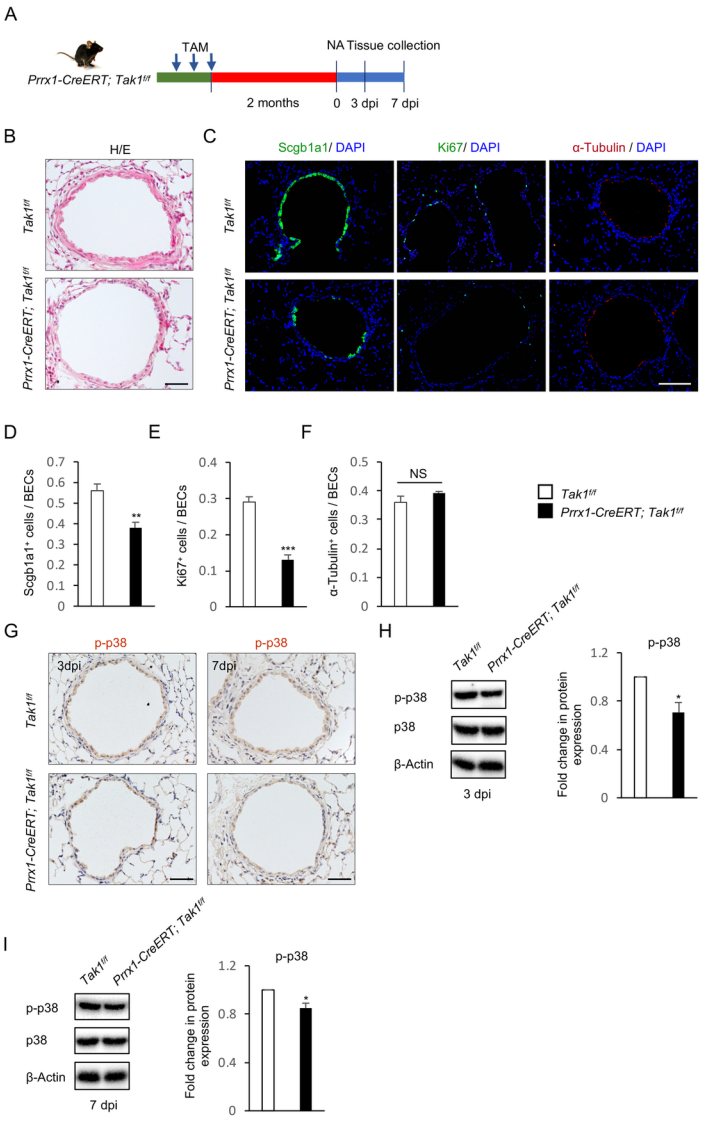

STEM_3125_Figure-6.tif

Figure 7

Huijuan Liu

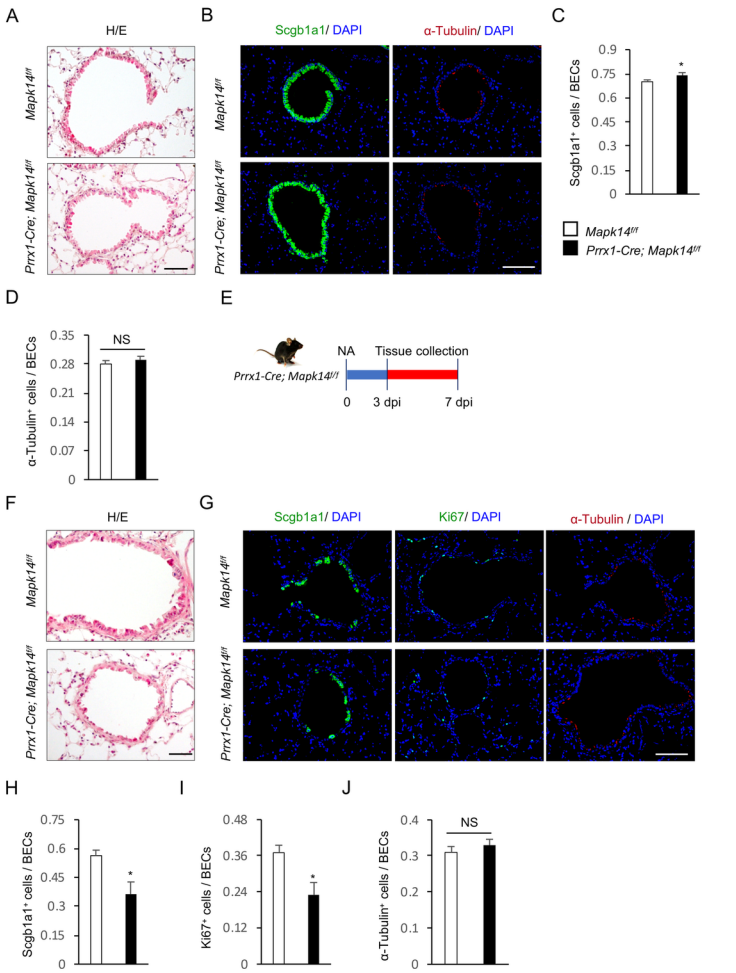

STEM_3125_Figure-7.tif

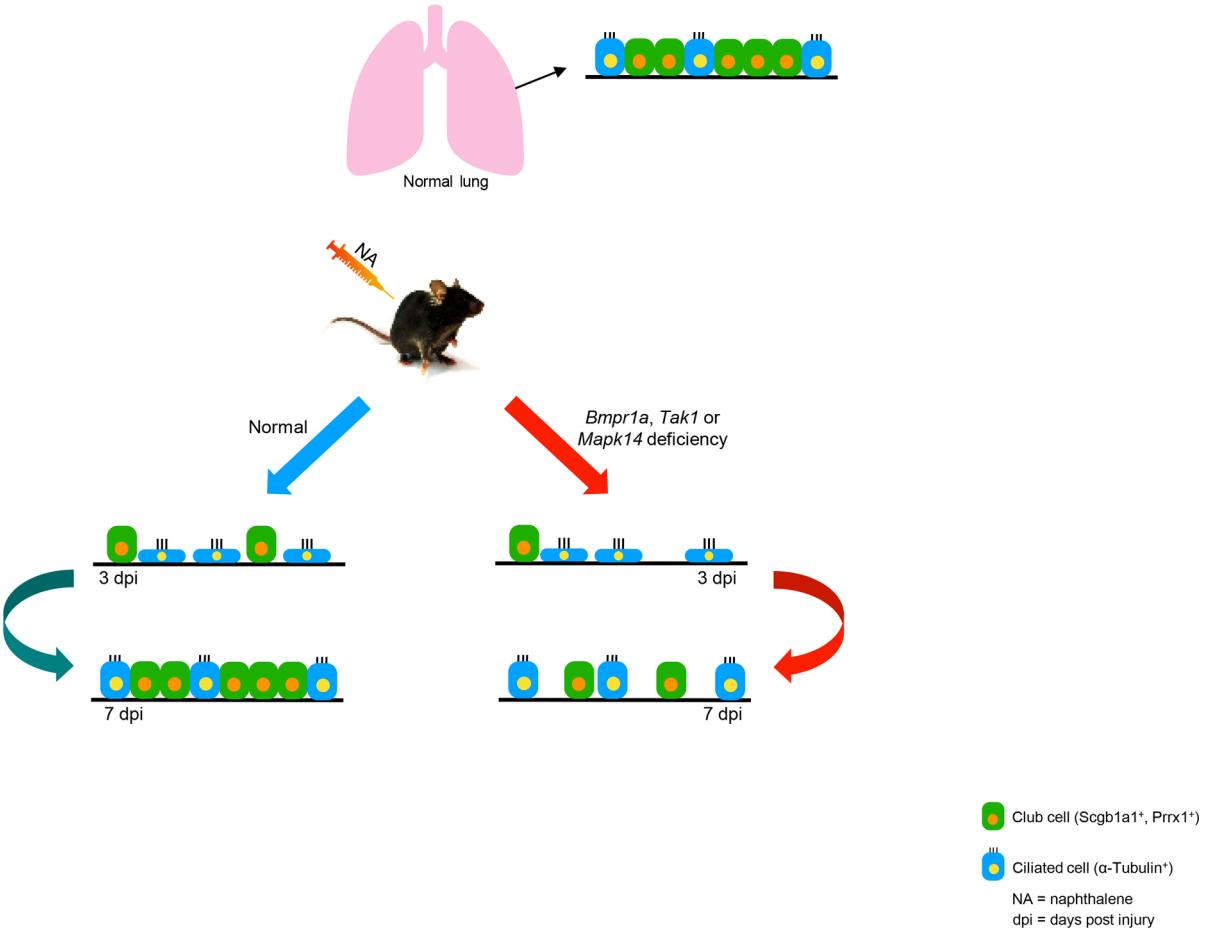

STEM_3125_Graphical abstract.tif